Gating Dynamics of the Acetylcholine Receptor Extracellular Domain

Sudha Chakrapani, Timothy D. Bailey, and Anthony Auerbach

Center for Single-Molecule Biophysics and Department of Physiology and Biophysics, State University of New York at Buffalo, Buffalo, NY 14214

ABSTRACT We used single-channel recording and model-based kinetic analyses to quantify the effects of mutations in the extracellular domain (ECD) of the α-subunit of mouse muscle–type acetylcholine receptors (AChRs). The crystal structure of an acetylcholine binding protein (AChBP) suggests that the ECD is comprised of a β-sandwich core that is surrounded by loops. Here we focus on loops 2 and 7, which lie at the interface of the AChR extracellular and transmembrane domains. Side chain substitutions in these loops primarily affect channel gating by either decreasing or increasing the gating equilibrium constant. Many of the mutations to the β-core prevent the expression of functional AChRs, but of the mutants that did express almost all had wild-type behavior. Rate-equilibrium free energy relationship analyses reveal the presence of two contiguous, distinct synchronously-gating domains in the α-subunit ECD that move sequentially during the AChR gating reaction. The transmitter-binding site/loop 5 domain moves first ($\Phi = 0.93$) and is followed by the loop 2/loop 7 domain ($\Phi = 0.80$). These movements precede that of the extracellular linker ($\Phi = 0.69$). We hypothesize that AChR gating occurs as the stepwise movements of such domains that link the low-to-high affinity conformational change in the TBS with the low-to-high conductance conformational change in the pore.

KEY WORDS: nicotinic • single channel • kinetics • REFER

INTRODUCTION

Nicotinic acetylcholine receptors (AChRs) are members of the ligand-gated ion channel superfamily and mediate fast neurotransmission at cholinergic synapses (Changeux and Edelstein, 1998; Colquhoun and Sakmann, 1998; Corringer et al., 2000; Unwin, 2000; Karlin, 2002). These allosteric proteins are composed of five homologous subunits ($\alpha_2\beta\delta\varepsilon$ at the adult nerve-muscle synapse). Each subunit has two distinct modules—an extracellular domain (ECD) that in the α-subunit contains the "+" side of the transmitter-binding site (TBS), and a transmembrane domain (TMD) that forms the ion-conducting pore. The TBS and the middle of the TMD are separated by ~50 Å (Fernando Valenzuela et al., 1994; Miyazawa et al., 1999). The presence of a suitable ligand (i.e., an agonist) at the TBS triggers a concerted, global change in the protein's conformation that results in an increased agonist affinity of the TBS and an increased ionic conductance of the pore. The dynamics of the ECD during this "gating" reaction are the topic of this report.

The structure of the AChR ECD is homologous to that of the acetylcholine binding protein (AChBP) (Brejc et al., 2001). The core of AChBP consists of a hydrophobic β-sandwich with individual β-strands connected by short stretches of hydrophilic amino acids (loops, numbered 1–10). Three of these loops in the AChR α-subunit are located on the "+" side of the subunit interface between the TBS and the membrane (Fig. 1). Loop 2 bridges β-strands 1 and 2, loop 5 links β-strands 4 and 5 and contains binding segment A (Galzi et al., 1990), and loop 7 spans β-strands 6 and 7 and is also known as the "cys-loop" (Fig. 1).

Functional and structural studies suggest that these loops participate in relaying the allosteric conformational change between the TBS and the TMD. In loop 5, which is near a central tryptophan residue in the TBS, mutations can cause substantial increases in the diliganded gating equilibrium constant but have little or no effect on agonist binding or desensitization (Chakrapani et al., 2003). Because a change in equilibrium constant after a perturbation indicates a local movement, these studies suggest that loop 5 moves between "closed" and "open" conformations. Kinetic analyses of AChRs having mutation to loop 5 residues suggest that this region moves early and synchronously with the TBS during diliganded gating. Loop 2, loop 7, and the extracellular linker (EL; part of which includes the M2 transmembrane helix; Horenstein et al., 2001; Miyazawa et al., 2003) form the interface of the ECD and the TMD. Mutations of these regions alter the

Address correspondence to Anthony Auerbach, Center for Single-Molecule Biophysics and Department of Physiology and Biophysics, State University of New York at Buffalo, Buffalo, NY 14214. Fax: (716) 829-2569; email: auerbach@buffalo.edu

Abbreviations used in this paper: AChR, acetylcholine receptor; ECD, extracellular domain; EL, extracellular linker; REFER, rate-equilibrium free energy relationship; TMD, transmitter domain; TBS, transmitter-binding site.

J. Gen. Physiol. © The Rockefeller University Press • 0022-1295/2004/04/341/16 $8.00
Volume 123 April 2004 341–356
http://www.jgp.org/cgi/doi/10.1085/jgp.200309004

AChR gating equilibrium constant (Grosman et al., 2000a; Shen et al., 2003) and increase the agonist EC_{50} in the related glycine (Schofield et al., 2003) and $GABA_A$ receptors (Kash et al., 2003). Thus, it is certain that α-subunit residues in loop 2, loop 7, and the EL/M2 move during gating. Kinetic analyses of AChRs having mutations to an EL/M2 residue suggest that this region moves later than the TBS during diliganded gating.

There have been two proposals regarding the roles of these three regions in the gating reaction mechanism. First, it has been suggested that an intramolecular, electrostatic interaction between loop 2, loop 7, and the EL/M2 is an important element that couples changes between the "closed" and "open" conformations specifically in $GABA_A$ receptors (Kash et al., 2003). Second, Unwin and coworkers interpreted electron microscope images of *Torpedo* AChR (in alignment with AChBP) as indicating that the allosteric conformational change involves a 15° rotation of the inner β-sheets that is communicated to the TMD through a hydrophobic interaction between loop 2 and the EL/M2 (Unwin et al., 2002; Miyazawa et al., 2003). Loop 7 is of particular interest because it is the signature "cys-loop" that defines membership in the pentameric-receptor channel superfamily. A mutation in loop 7 in the AChR α-subunit has been shown to alter both binding and gating kinetics (Shen et al., 2003), and studies in the $GABA_A$ receptor α_1-subunit suggests the involvement of the central D residue in the proposed electrostatic interaction with residues in loop 2 and the EL/M2 (Kash et al., 2003).

We have coupled mutational studies with single-channel kinetic analyses in order to further identify regions in the ECD of the AChR α-subunit that participate in the gating conformational change. Our results (summarized in Fig. 14) suggest that the ECD is organized into distinct, dynamic gating modules that move sequentially, as a linked system, during diliganded gating.

MATERIALS AND METHODS

Expression and Mutagenesis

Mouse AChRs were expressed in human embryonic kidney cells (HEK 293) by transfection with calcium phosphate. cDNA clones of α, β, δ, and ε subunits in pRBG4 were used in the subunit ratio 2:1:1:1, respectively. The medium was changed 24 h after the addition of DNA and electrophysiological recordings began another 24 h later. All mutations were made using the QuikChange™ site-directed mutagenesis kit (Stratagene) and were confirmed by dideoxy sequencing.

Single-channel Recordings and Kinetic Analysis

Patch-clamp recordings were done in the cell-attached configuration. Pipettes were pulled from borosilicate capillaries, coated with Sylgard (Dow Corning) and fire polished to a resistance of 10–15 MΩ. Dulbecco's phosphate buffered saline-PBS (mM: 137 NaCl, 0.9 $CaCl_2$, 2.7 KCl, 1.5 KH_2PO_4, 0.5 $MgCl_2$, and 8.1 Na_2HPO_4, pH 7.3) was used in the bath. The pipette solution contained PBS plus agonist. The potential of the pipette was held at +70 mV, which in the cell-attached configuration corresponds to a membrane potential of ≈100 mV. Single-channel currents were recorded using an Axopatch 200B amplifier (Axon Instruments, Inc.). The data were digitized at a sampling rate of 100 kHz after low-pass filtering to 20 kHz (8-pole Bessel).

All kinetic analyses were done using QuB software (www.qub.buffalo.edu). Idealization of the currents into noise-free intervals was done using the segmental k-means algorithm (SKM) at full bandwidth with a C↔O model (both rate constants = 100 s^{-1}), or by a half-amplitude threshold-crossing algorithm after additional low-pass filtering to 2–5 kHz. Clusters of openings corresponding to a single channel were defined as a series of open intervals separated by closed intervals, all of which were shorter than a critical duration, τ_{crit}, which was defined using a method that minimizes the total number of misclassified events (Jackson et al., 1983). Model-based kinetic analyses of the idealized intervals were done using a maximum interval likelihood method (Qin et al., 1996), with an imposed dead time of 25–50 μs.

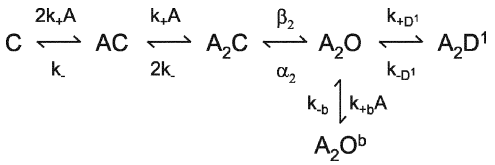

SCHEME I

Scheme I was used to model the sequences of interval dwell-times within clusters. A is the agonist and A_2C (closed) and A_2O (open) represent the endpoints of the diliganded gating reaction. AChRs in the A_2C conformation have a low agonist affinity (∼150 μM for ACh) and a low ionic conductance (essentially zero), while those in the A_2O conformation have a high agonist affinity (∼10 nM for ACh) and a high ionic conductance (∼70 pS in physiological solutions). D stands for desensitized, which reflects an AChR having a high agonist affinity (like O) but is, for some undefined reason, nonconducting (like C; Auerbach and Akk, 1998). The superscript "b" stands for channel-blocked, which also represents a high-affinity, nonconducting AChR, because of open-channel block by the agonist molecule.

The estimated ligand-binding rate constants were k_+ and k_-, which are the agonist association and dissociation rate constants pertaining to a single TBS. In our preparation the two TBS have essentially the same agonist affinity (Salamone et al., 1999). The estimated gating rate constants were β_2 and α_2, which are the channel-opening and -closing rate constants for diliganded AChRs. The equilibrium constants for binding and gating were calculated from the ratios of the rate constants ($K_d = k_-/k_+$ and $L_2 = \beta_2/\alpha_2$).

To ascertain whether a mutation increased or decreased the probability of channel opening (or had no effect), we examined currents activated by 30 μM ACh, which is approximately the EC_{50} (cluster $P_{open} \approx 0.5$) for wt AChRs. For more extensive kinetic modeling, interval durations were also obtained at several different concentrations of ACh and were fitted jointly by Scheme I, i.e., one set of rate constants for all concentrations with k_+ scaled linearly by the agonist concentration. The number of clusters that were recorded from each patch depended on the expression level of that particular construct. The number of interval durations at each concentration ranged from 478 to 95,034 (average = 27,231). In many cases we sought to estimate only the diliganded gating rate constants. Accordingly, we used a saturating concentration of agonist (20 mM choline or 1–2 mM ACh, which is >5-times higher than the respective K_d) so that the intervals within clusters mainly arose from gating rather than binding events.

We find it difficult to estimate activation rate constants for constructs in which the average lifetime of A_2C (~10 μs) is shorter than our time resolution (≥25 μs). Wild-type AChRs activated by ACh fall into this category (Maconochie and Steinbach, 1998). Therefore, in order to study constructs which had even larger opening rate constants with ACh we used the weak agonist choline, which supports (in wt AChRs) a diliganded gating equilibrium constant that is 500-times smaller than ACh (Zhou et al., 1999; Grosman and Auerbach, 2000a).

For both ACh and choline the saturating concentrations that we used are approximately equal to the equilibrium dissociation constant for (fast) open-channel block by the agonist at −100 mV (Auerbach and Akk, 1998; Grosman and Auerbach, 2000a). Thus, because of unresolved channel block, the single-channel current amplitudes were decreased and the apparent open-channel lifetimes were increased by ~2-fold. To estimate the true channel-closing rate constant, we measured the inverse of the open-channel lifetimes of AChRs activated by a low concentration of agonist (1 μM ACh and 400 μM choline), where channel-block was negligible. Further, to correct for choline dissociation from open AChRs, we subtracted a value of 200 s^{-1} from the closing rate constant estimate (Cymes et al., 2002). No such correction was needed for ACh because its dissociation from open AChRs is negligible compared with the closing rate constant (Grosman and Auerbach, 2001).

RESULTS

Loop 2

Loop 2 is composed of residues 45–48 in the mouse α-subunit (EVNQ; Fig. 1 and Table I). We examined the consequences of point mutations at three of these four residues with regard to both the ligand-binding and channel-gating rate and equilibrium constants.

TABLE I

Sequence Alignment of Loop 2

	* *
AChBP	NEITNE
M.α1AChR	DEVNQI
M.α2AChR	DEKNQM
M.α3AChR	DEVNQI
M.α4AChR	DEKNQM
M.α5AChR	DEKNQL
M.α6AChR	DEVNQI
M.α7AChR	DEKNQV
M.β1AChR	NEKDEE
M.β2AChR	DEKNQM
M.β3AChR	DEKNQL
M.β4AChR	NEREQI
M.ϵ1AChR	NEKEET
M.δ1AChR	LENNND
B.α1AChR	NEKEET
T.α1AChR	DEVNQI
X.α1AChR	DEVNQI
R.α1AChR	DEVNQI
H.α1AChR	DEVNQI
H.α1GABA	SDHDME
H.α1Gly	AETTMD
H.α5HT	DEKNQV

Sequence alignment of loop 2 in AChBP and subunits from pentameric, "cys-loop" receptor-channels. The line marks loop 2 in AChBP. The * marks the putative beginning and end of loop 2. In the alignment, M denotes mouse, B, bovine; T, *Torpedo*; X, *Xenopus*; R, rat; and H, human.

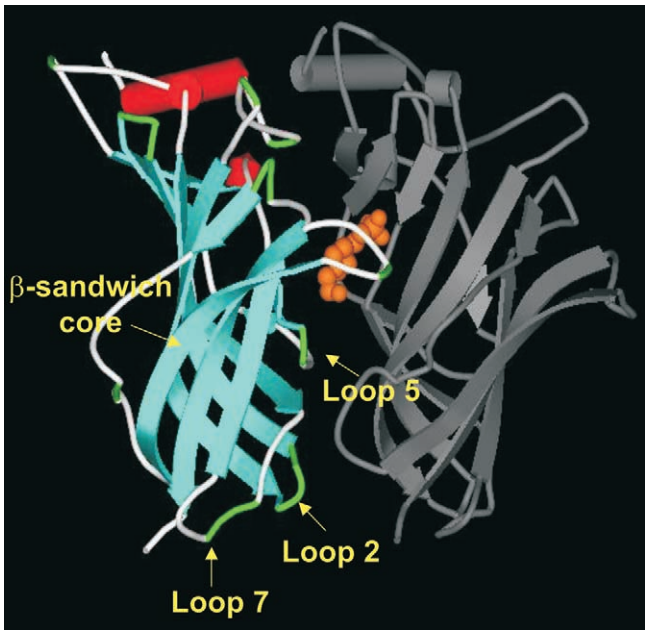

FIGURE 1. Location of loops 2, 5, 7, and the β-sandwich core in AChBP. The AChBP subunit interface is shown perpendicular to the pseudo-fivefold axis of symmetry. A HEPES molecule in the transmitter binding site is shown in orange. The AChR α-subunit corresponds to the "+"-side of this interface (cyan). Loop 2 and 7 are at the interface of the extracellular and transmembrane domains.

Fig. 2 shows currents elicited by 30 μM ACh in wt and five V46 mutant AChRs. V46I modestly increased the cluster open probability (P_{open}), V46A, V46E, V46M, and V46Y significantly decreased this parameter. Using a saturating concentration of choline as the agonist, we found that V46I increased the diliganded gating equilibrium constant (L_2), mainly by increasing the channel opening rate constant (Table II). Because the A, E, M, and Y substitutions decreased P_{open} they were studied further using ACh as the agonist (Fig. 3 and Table III). The M and Y substitutions decreased L_2 (5.5- and 8.7-fold, respectively) mainly by decreasing the channel opening rate constant. V46M did not affect the ACh association or dissociation rate constants, while V46Y caused a small (2.7-fold) decrease in the agonist dissociation rate constant.

For the A and E mutants, L_2 was very small and at ACh concentrations <400 μM the currents were not organized into well-defined clusters. This prevented us from using model-based kinetic analyses to estimate the agonist association and dissociation rate constants. However, by using low and saturating concentrations of ACh we were able to estimate the channel-closing and

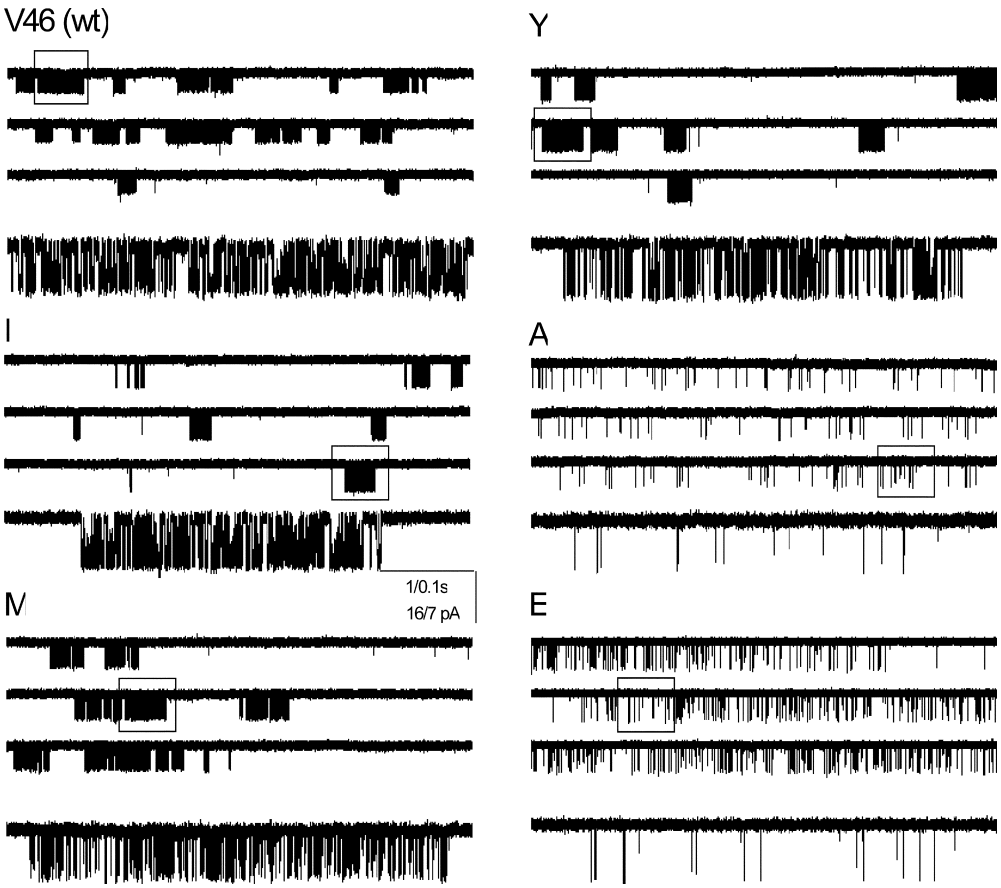

FIGURE 2. αV46 in loop 2: single-channel currents. For each panel the top three current traces are continuous and the boxed region is shown below at a higher time-resolution (30 μM ACh; open is down; filtered at 10 kHz for display). All mutations decreased the cluster P_{open} except I. The effects on cluster P_{open} were mainly due to a change in the lifetime of closed-intervals (Table II).

-opening rate constants respectively, and their ratio, L_2. As was the case for the other mutations, the A and E substitutions changed L_2 (77- and 200-fold decreases, respectively) mainly by altering the channel-opening rate constant (Table II).

The adjacent loop 2 residue, N47, was mutated to D, L, K, and A (Fig. 4). Two of these perturbations (D and L) decreased and two (K and A) increased L_2. For the D and L constructs we were able to estimate both ACh-binding and channel-gating parameters (Fig. 5). These substitutions did not significantly alter the rate constants for ACh association/dissociation to resting AChRs, but they decreased L_2 (5.3- and 9.0-fold), predominantly by decreasing the opening rate constant (Table II and 3).

TABLE II

Gating Rate Constants for Loop 2 Constructs

αloop 2	Construct	$\beta_2^{Choline}$	$\alpha_2^{Choline}$	β_2^{ACh}	α_2^{ACh}	L_2 ratio
		s^{-1}	s^{-1}	s^{-1}	s^{-1}	
	Wt	100	2,100	50,000	2,000	1.000
V46	I	249	1,982	—	—	2.638
	M	—	—	31,129	6,873	0.181
	Y	—	—	6,921	2,399	0.115
	A	—	—	1,340	4,135	0.013
	E	—	—	795	6,613	0.005
N47	A	933	1,450	—	—	13.396
	K	607	2,371	—	—	5.333
	D	—	—	16,124	3,420	0.189
	L	—	—	8,717	3,140	0.111
Q48	K	—	—	9,469	9,912	0.038
	A	2,836	10,271	—	—	5.787
	V	NFC				

The diliganded channel-opening ($\beta_2^{Choline}$) and -closing ($\alpha_2^{Choline}$) rate constants for choline were estimated from single-channel currents elicited by 20 and 0.4 mM choline, respectively. The opening (β_2^{ACh}) and closing (α_2^{ACh}) rate constants for ACh were estimated from model-based kinetic analysis of clusters elicited at different concentrations of ACh. The diliganded gating equilibrium constant L_2 was calculated as the ratio β_2/α_2. "L_2 ratio" is the ratio of L_2 for the mutation and the wild-type. NFC denotes no functional channels either due to loss of expression or function or both.

TABLE III

Binding Equilibrium Constants of Loop 2 Constructs Activated by ACh

αloop 2	Construct	k_+	k_{-1}	K_d
		$\mu M^{-1}\, s^{-1}$	s^{-1}	μM
	wt	167 ± 2	24,745 ± 257	148
V46	M	117 ± 2	13,882 ± 244	119
	Y	209 ± 9	11,320 ± 509	54
N47	D	145 ± 4	20,014 ± 577	138
	L	116 ± 4	16,106 ± 550	139
Q48	K	169 ± 5	10,138 ± 369	60

The binding and gating rate constants were estimated by globally fitting interval durations from different concentrations of ACh using Scheme I (see Figs. 3 and 8). K_d was calculated as the ratio k_-/k_+. The K_d for ACh on wt receptors is from (Zhou et al., 1999).

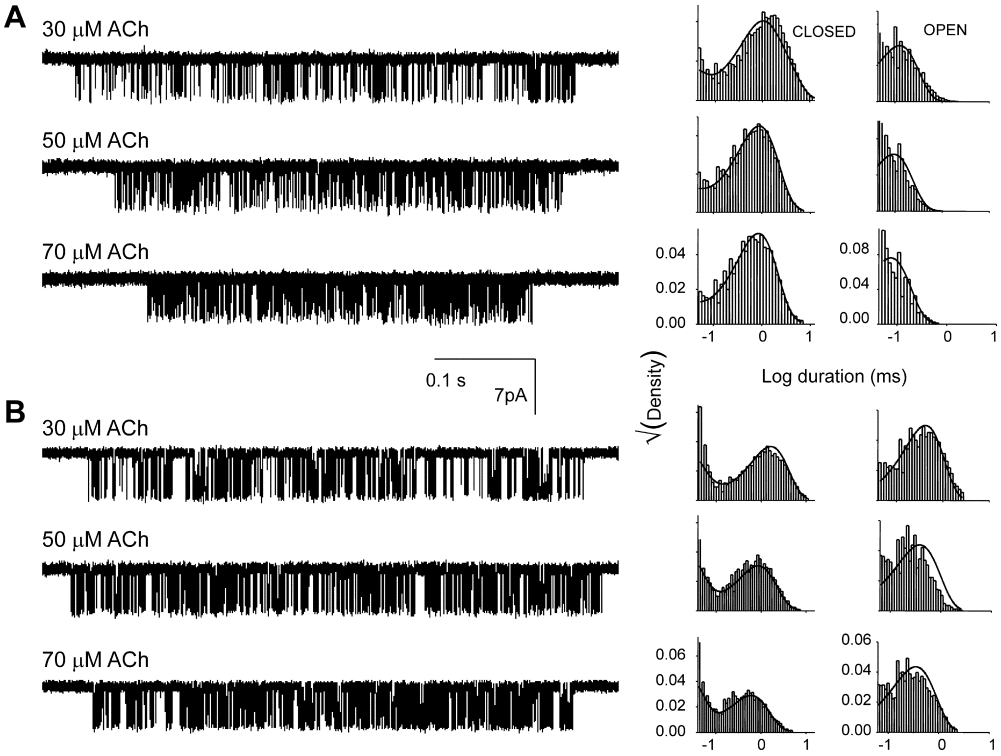

FIGURE 3. αV46: kinetic analysis across concentrations. (A) αV46M. (B) αV46Y. For each construct single-channel currents (left) and interval duration histograms (right) elicited by different ACh concentrations (30, 50, and 70 μM, top to bottom) are shown. The solid lines are probability density functions calculated from the rate constants of Scheme I obtained from a joint fit across all concentrations. Neither of these mutations had a significant effect on agonist binding to closed AChRs (Table III).

The K and A constructs increased L_2 and were therefore studied in the presence of choline. In these mutants the channel opening rate constants were ~6- and ~9-fold faster than the wt, respectively (Table II). A plot of the physicochemical properties of the mutant side chain versus L_2 shows that for αN47 there is no apparent correlation between side chain hydrophobicity or volume and the observed effect on the gating equilibrium constant (Fig. 6). For residue αV46 there was a tendency for constructs with more polar side chains to have smaller L_2-values.

At the next loop 2 residue, Q48, we examined three side chain substitutions (Fig. 7 A). The K substitution decreased L_2 ~26-fold, mainly by reducing the channel-

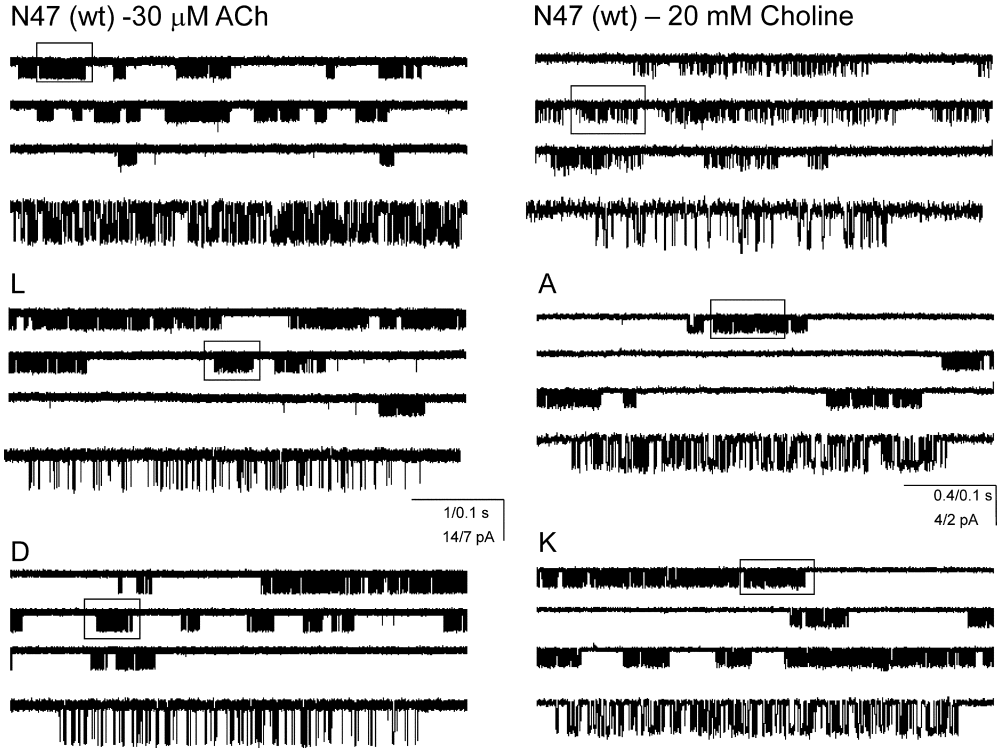

FIGURE 4. αN47 in loop 2: single-channel currents. For each panel the top three current traces are continuous and the boxed region is shown below at a higher time-resolution. The L and D mutations (30 μM ACh) decreased the cluster P_{open}, whereas the A and K mutations (20 mM choline) increased the cluster P_{open} (filtered at 2 kHz for display). For both classes of mutation the effect on cluster P_{open} was mainly due to a change in the closed-interval lifetime (Table II).

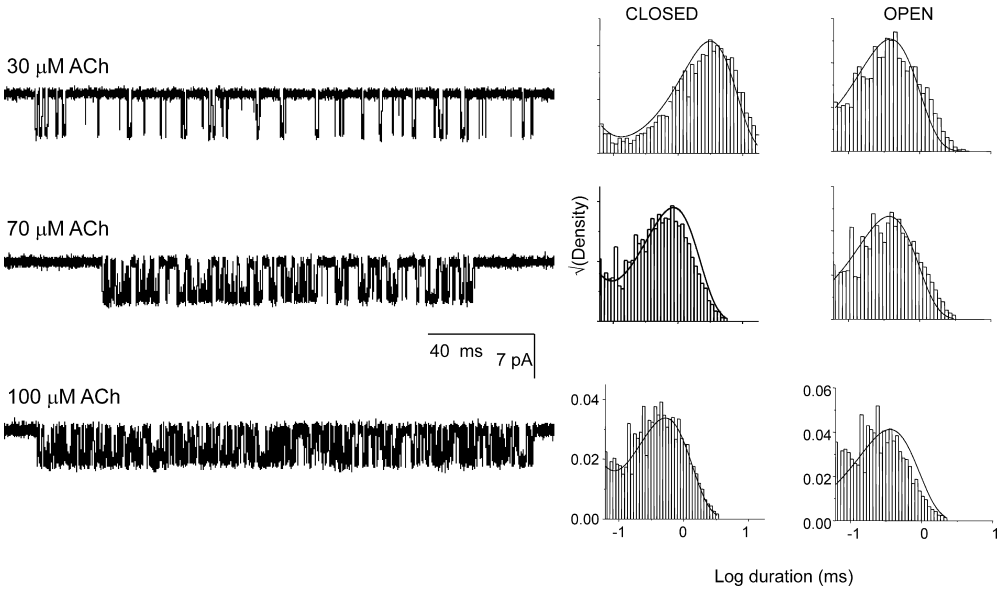

FIGURE 5. αN47D: kinetic analysis across concentrations. Representative clusters and dwell time histograms, with superimposed probability density functions calculated from the rate constants of Scheme I obtained from a joint fit across all concentrations. This mutation had no effect on ACh association or dissociation to closed AChRs (Table III).

opening rate constant. This mutation did not alter the agonist association rate, but it caused a modest, ~2.5-fold decrease in the agonist dissociation rate constant (Fig. 8 and Table III). The V substitution led to a complete loss of activity (no openings were apparent in >30 patches at various agonist concentrations using both choline and ACh; unpublished data). Apparently, this mutant prevents AChR expression, gating, or both. Finally, the A substitution increased L_2 by ~6-fold (Fig. 7 B and Table II). However, in this latter construct both the channel-opening and -closing rate constants were greater than the wt. This behavior is unusual and is discussed in more detail, below. None of the loop 2 mutants had any significant effect on AChR desensitization.

To summarize, the loop 2 point substitutions either increased or decreased gating, but had little or no effect on agonist binding or desensitization. Of the 12 mutant constructs that we studied, the maximum change in the gating equilibrium constant was ~200-fold, which pertains to AChRs having both α-subunit residues mutated. In all the mutants that we investigated the change in the gating equilibrium constant was mainly caused by a change in the channel-opening rate constant.

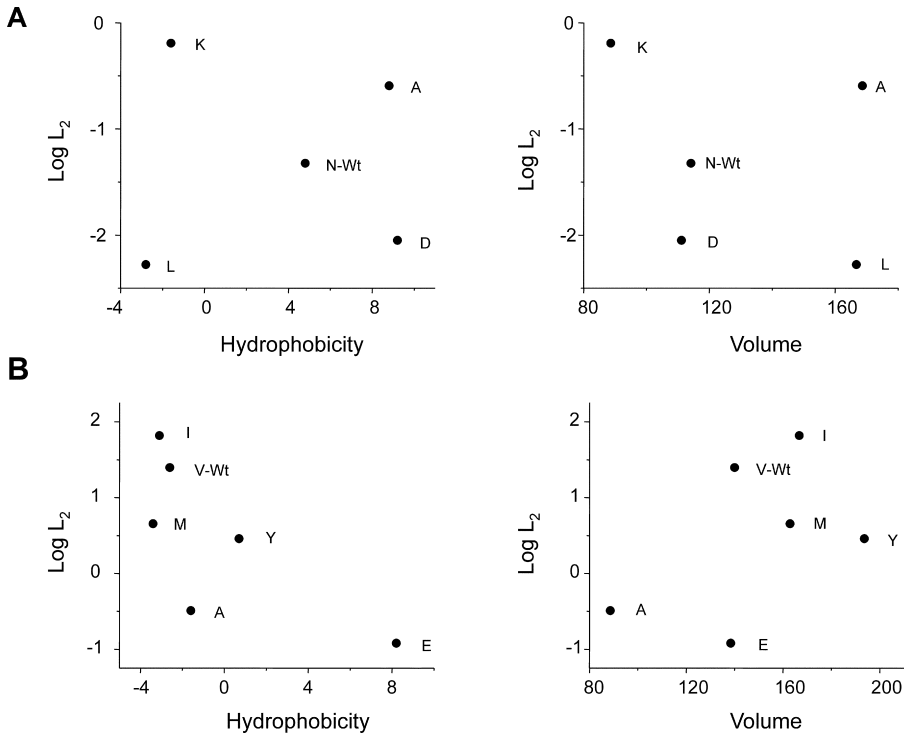

FIGURE 6. The diliganded gating equilibrium constant is not strongly correlated with the chemical properties of the sidechains at αN47 and αV46. (A) At positions αN47 there is no correlation between side-chain hydrophobicity or volume and the effect on the diliganded gating equilibrium constant (L_2). (B) At positions αV46, there is some apparent correlation between side-chain hydrophobicity and L_2, which decreases with increasing side-chain polarity.

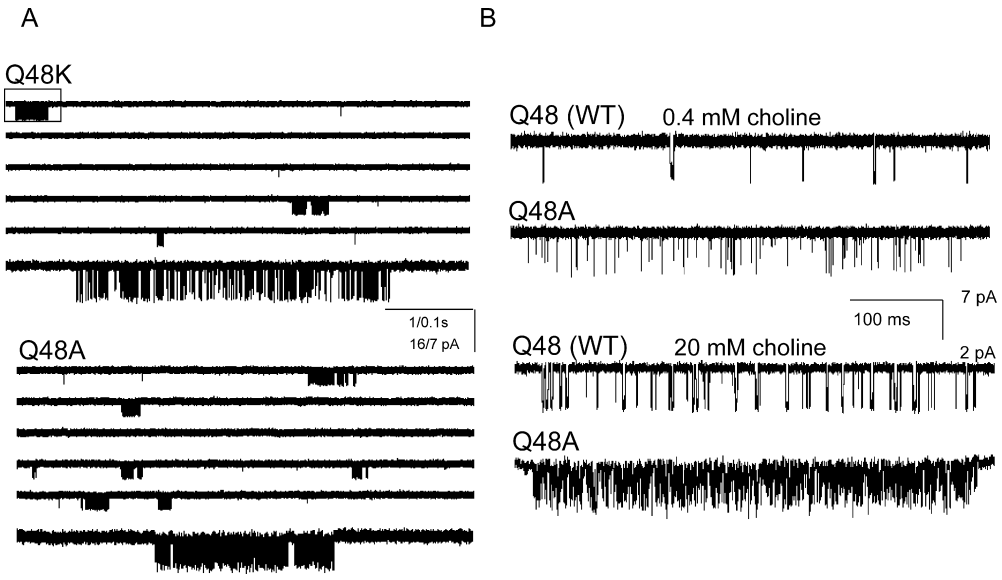

FIGURE 7. αQ48 in loop 2: single-channel currents. (A) Example clusters elicited by 30 μM ACh. The αQ48K substitution decreased the cluster P_{open} mainly by increasing the closed-interval lifetimes. The αQ48A substitution increased the cluster P_{open}, but both the closed and open interval lifetimes decreased (a "catalytic" effect). (B) Representative clusters from wt and αQ48A AChRs at low and high concentrations of choline. The A substitution increases L_2 (Table II).

Loop 7

Loop 7 is the 13-residue "cys-loop" (C-X_{13}-C) that is the hallmark of membership in the pentameric family of ligand-gated ion channels. The two flanking cysteine residues form a disulfide bond that binds the β-sandwich core (Brejc et al., 2001). The central residues of loop 7, FPFD, are highly conserved among receptor subunits (Table IV). We studied the effects of side-chain substitutions at the D position in this motif (α138) and at five other loop 7 positions (Fig. 9). Three of the mutant constructs did not express functional channels or led to complete loss of activity (F137A, D138A, D138K; unpublished data), three modestly increased L_2, and the remaining four decreased L_2. However, in only two of these constructs, F135A and Q140A, were the changes in L_2 substantial (>5-fold) (Table V).

We were able to measure ACh association and dissociation rate constants in three loop 7 mutants (Fig. 10 and 11, and Table VI). In all cases, the change in K_d was <2.5-fold. We also did not detect an effect of any of the loop 7 substitutions on desensitization.

The two mutants that showed large effects on gating were F135A and Q140A. F135 is the initial residue of

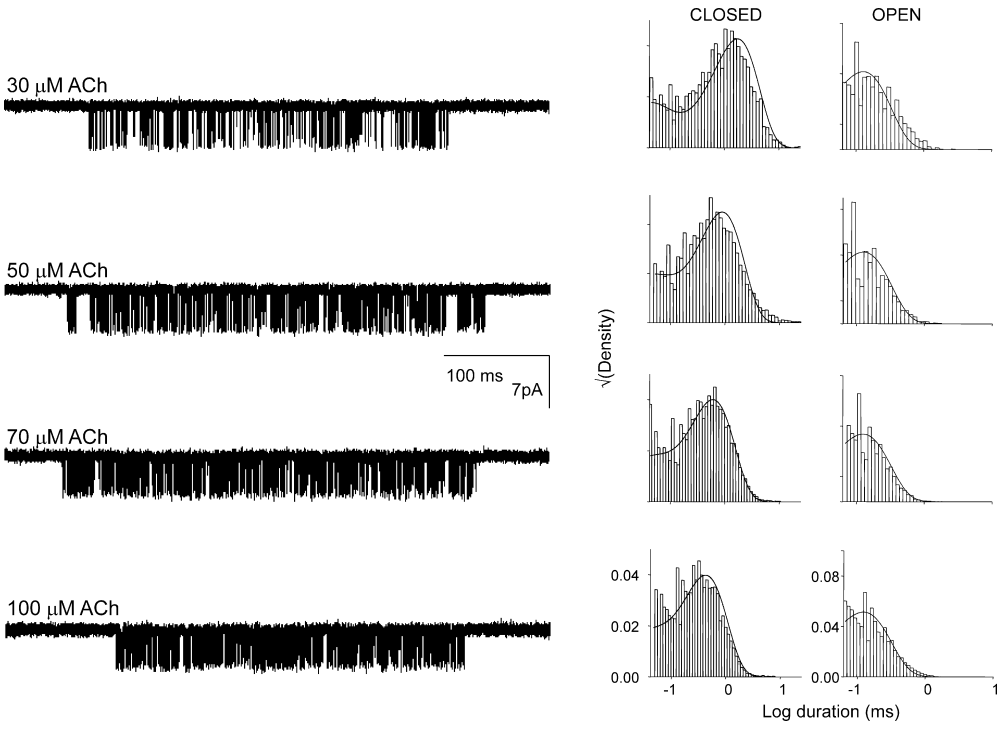

FIGURE 8. αQ48K: kinetic analysis across concentrations. Representative clusters and dwell time histograms, with superimposed probability density functions calculated from the rate constants of Scheme I obtained from a joint fit across all concentrations. This mutation did not have a significant effect on ACh association or dissociation to closed AChRs (Table III).

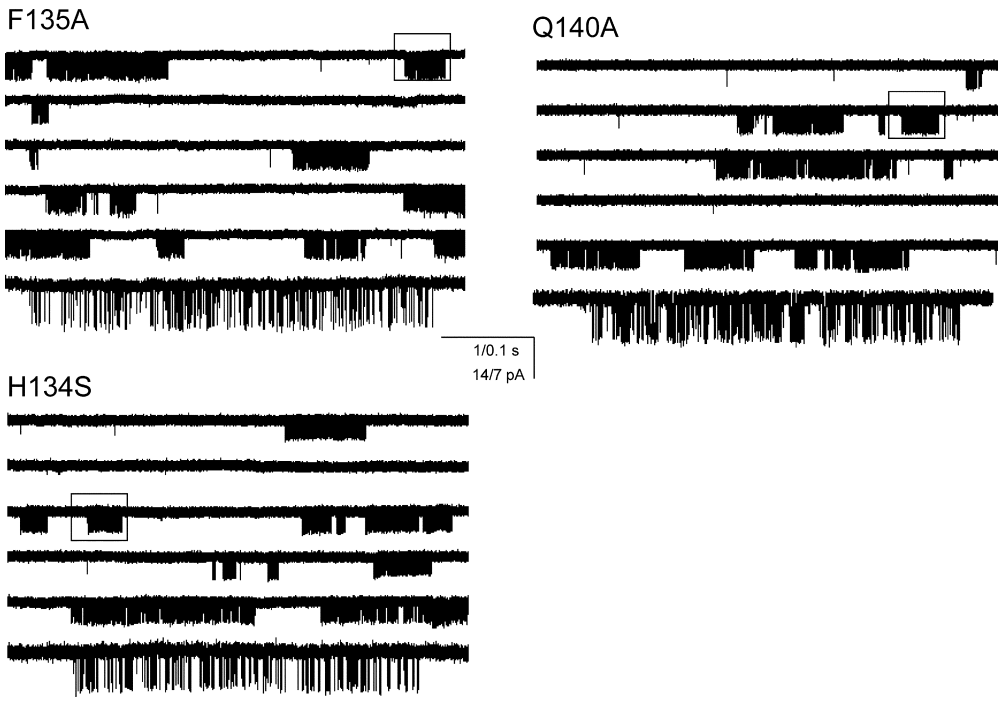

FIGURE 9. Loop 7: single-channel currents. For each panel the top three current traces are continuous and the boxed region is shown below at a higher time-resolution. These mutations decreased cluster P_{open} (30 μM ACh) mainly by increasing the closed-interval lifetimes (Table V).

the FPFD motif and is strictly conserved in all AChRs and other members of the superfamily. For the A substitution, the open interval distributions (at all concentrations of ACh) were unusual because they had two distinct kinetic components (Fig. 11 A). This indicates the presence of two open states. We extended Scheme I accordingly, by connecting a second open state, in turn, to each of the other states (except A_2O^b) in the model. The result was that one scheme, in which the two open states were each connected to the diliganded closed state A_2C, consistently produced a log likelihood that was >10 units greater than with the other schemes. We therefore conclude that in F135A there are two, uncou-

TABLE IV
Sequence Alignment of Loop 7

	*	*
AChBP	SCDVSGVDTESG-ATCR
M.α1AChR	YCEIIVTHFPFDEQNCS
M.α2AChR	SCSIDVTFFPFDQQNCK
M.α3AChR	SCKIDVTYFPFDYQNCT
M.α4AChR	SCSIDVTFFPFDQQNCT
M.α5AChR	SCTIDVTFFPFDLQNCS
M.α6AChR	SCPMDITFFPFDHQNCS
M.α7AChR	SCYIDVRWFPFDVQQCK
M.β1AChR	SCSIQVTYFPFDWQNCT
M.β2AChR	SCSIDVTFFPFDQQNCK
M.β3AChR	SCTMDVTFFPFDRQNCS
M.β4AChR	ACKIEVKHFPFDQQNCT
M.ϵ1AChR	TCAVEVTYFPFDWQNCS
M.δ1AChR	SCPISVTYFPFDWQNCS
B.α1AChR	YCEIIVTGFPFDEQNCS
T.α1AChR	YCEIIVTHFPFDQQNCT
X.α1AChR	YCEIIVTYFPFDQQNCS
R.α1AChR	YCEIIVTHFPFDEQNCS
H.α1AChR	YCEIIVTHFPFDEQNCS
H.α1GABA	ECPMHLEDFPMDAHACP
H.α1Gly	ACPMDLKNFPMDVQTCI
H.α5HT	ACSLDIYNFPFDVQNCS

Sequence alignment of loop 7 in AChBP and subunits from pentameric, "cys-loop" receptor-channels. The line marks loop 7 in AChBP. The * marks the putative beginning and end of loop 7. In the alignment, M denotes mouse; B, bovine; T, torpedo; X, *Xenopus*; R, rat; and H, human.

TABLE V
Gating Rate Constants for Loop 7 Constructs

αloop 7	Construct	$\beta_2^{Choline}$	$\alpha_2^{Choline}$	β_2^{ACh}	α_2^{ACh}	L_2 ratio
			s^{-1}	s^{-1}	s^{-1}	
	WT	100	2,100	50,000	2,000	1.000
H134	S			18,474	2,506	0.295
F135	A	—	—	1,145	5,486	0.008
F137	M	225	1,017	—	—	4.609
	A	NFC				
D138	E	239	1,456	—	—	3.420
	A	NFC				
	K	NFC				
Q140	A	—	—	2,650	2,789	0.038
	L			30,710	2,868	0.428
N141	V	260	1,389	—	—	3.899

The diliganded channel opening rate constants for choline were estimated from single-channel currents elicited by 20 and 0.4 mM choline, respectively. The opening rate constants for ACh were estimated from model-based kinetic analysis of clusters elicited at different concentrations of ACh. The L_2 was calculated as the ratio β_2/α_2. "L_2 ratio" is the ratio of L_2 for the mutation and the wild-type. NFC denotes no functional channels either due to loss of expression or function or both.

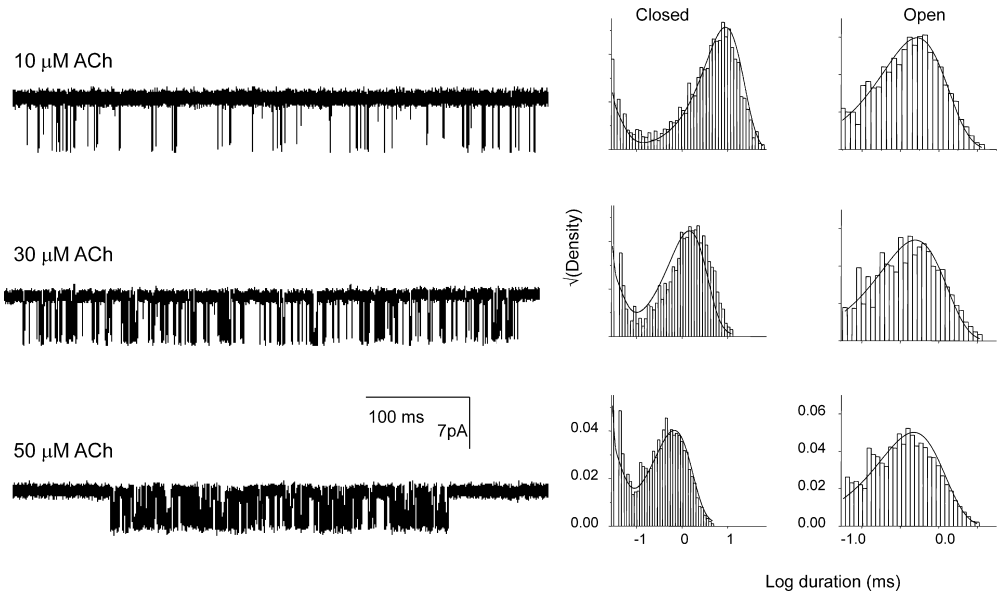

FIGURE 10. αH134S: kinetic analysis across concentrations. Representative clusters and dwell time histograms, with superimposed probability density functions calculated from the rate constants of Scheme I obtained from a joint fit across all concentrations. The αH134S mutant had no significant effect on agonist binding (Table VI).

pled gating reactions. Our kinetic analyses indicate that this mutation causes only a small (<2-fold) change in the ACh binding and desensitization rate constants, but a large (~125-fold) decrease in the (main) gating equilibrium constant, mainly because of a decrease in the channel-opening rate constant (Table V). The opening and closing rate constants for the secondary gating reaction were fivefold lower and 15-fold higher than wt.

At position Q140, an L substitution caused a small-but-measurable (~2-fold) decrease in gating, and had no effect on ligand-binding or desensitization (Table V and VI). Similar to F135A, Q140A exhibited two open states (Fig. 11 B). Again, a statistical analysis of various schemes indicated that the two open states are likely to each connect independently to state A_2C of Scheme I. In this construct, we detected a small decrease in the ACh dissociation rate constant but no change in the agonist association rate constant (Table VI). However, this mutation caused a large (26-fold) decrease in the gating equilibrium constant, mainly by reducing the open-

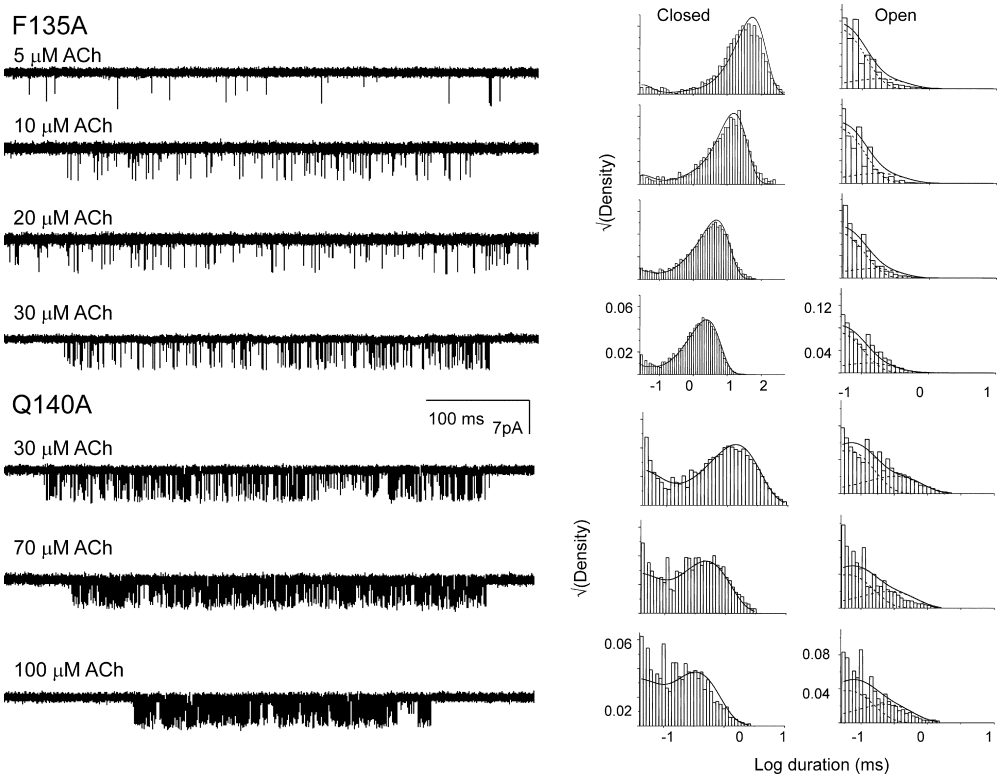

FIGURE 11. αF135A and αQ140A in loop 7 exhibit two open states. Example clusters elicited by the indicated ACh concentrations and their corresponding interval duration histograms. The histograms for the open-interval dwell times show two distinct components. The closed- and -open interval dwell times for all the concentrations were fitted jointly by a modified version of Scheme I in which a second open state was connected to the diliganded-closed state. Neither of these mutations had any significant effect on agonist binding (Table VI).

TABLE VI

Binding Equilibrium Constants of Loop 7 Constructs Activated by ACh

αloop 7	Construct	k_+	k_{-1}	K_d
		$\mu M^{-1}\ s^{-1}$	s^{-1}	μM
	wt	167 ± 2	24,745 ± 257	148
H134	S	269 ± 9	25,328 ± 860	94
F135	A	283 ± 7	21,355 ± 615	75
Q140	A	192 ± 3	11,461 ± 202	60
	L	104 ± 5	26,567 ± 1,567	255

The binding and gating rate constants were estimated by globally fitting interval durations from different concentrations of ACh using Scheme I (see Figs. 12 and 13). K_d was calculated as the ratio k_-/k_+. The K_d for ACh on wt receptors is from Zhou et al. (1999).

ing rate constant (Table V). The opening and closing rate constants for the secondary gating reaction were fourfold lower and 10-fold higher than wt.

To summarize, all but two of the loop 7 side-chain substitutions we investigated had only minor effects on the gating equilibrium constant, and several caused the loss of expression of functional AChRs. We did not detect a significant effect of any substitutions on ligand binding to the closed-conformation TBS or to desensitization. In the two loop 7 mutations that substantially increased L_2, a secondary diliganded gating reaction was apparent.

β-Strand Residues

A comparison of electron microscopic images of AChRs in the presence and the absence of agonist led Unwin et al. (2002) to suggest that there is an internal movement of the β-cores of the two α-subunits during gating. We studied 42 point-substitutions spread over 21 different positions on the β-strands and elsewhere in the α-subunit ECD (Table VII). Of these, about half ($n = 22$) had wt gating rate constants (<3-fold change) and about one-third ($n = 15$) resulted in loss of expression of functional channels. Three mutants had modestly increased the gating equilibrium constant, R20L (∼3.6-fold), L40A (∼4-fold), and A122L (∼3.5-fold).

The only position that showed a significant sensitivity with regard to gating was M144. We examined the kinetic behavior of eight different side chains at this position. The E/G/K substitutions led to complete loss of functional receptors and T/I/A substitutions had no measurable effect. M144L caused a ∼6.5-fold increase and M144S caused a ∼4.4-fold decrease in L_2 (Fig. 12). In both cases the effect was mainly by altering the opening rate constant. In M144S receptors (activated by ACh), the agonist association (130 $\mu M^{-1}s^{-1}$) and dissociation (22,019 s^{-1}) rate constants, and hence the equilibrium dissociation constant (169 μM), were the same as in wt AChRs.

REFER Analyses

We can interpret the rate constants for diliganded gating in the ECD mutants in the framework of rate-equilibrium free energy relationships (REFERs). When linear, the slope of this relationship, Φ, is an estimate of the extent to which the site of the perturbation has adopted its "open" structure at the transition state of the gating reaction (Grosman et al., 2000b). This, in turn, provides a map of the temporal sequence of residue motions during protein conformational change (Itzhaki et al., 1995; Villegas et al., 1998; Ternstrom et al., 1999; Grosman et al., 2000b).

A REFER analysis of loop 2 is shown in Fig. 13 A. We omitted Q48A from this plot because this substitution results in an increase in both the forward and the reverse rate constants for the gating reaction, which implies that for this case the underlying assumption of REFER analysis (that the energetic effect of a perturbation on the transition state is a linear combination of its effects on the ground states) was invalid. Thus, in Q48A there appears to be a "catalytic" effect of the A substitution that independently lowers the transition state energy. Substantial catalytic effects are rare, but not unprecedented, in AChR gating (Cymes et al., 2002).

The overall Φ-value for loop 2 is 0.806 ± 0.052. This indicates that loop 2 moves relatively early during the channel-opening process. The Φ-value for loop 2 is sig-

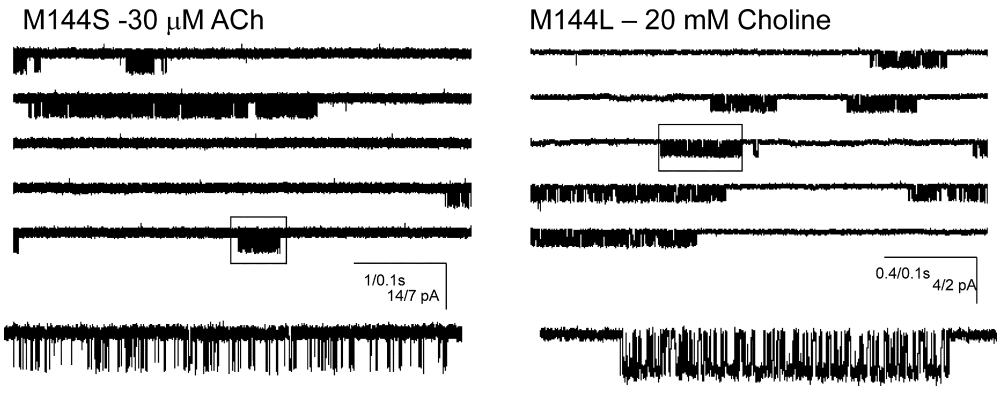

FIGURE 12. αM144: single-channel currents. Continuous traces showing clusters elicited by 30 μM ACh, with the boxed cluster shown below at a higher time-resolution. This residue is on strand β7 and is close to the disulfide bond that binds the β-sandwich core. αM144L increased cluster P_{open} while αM144S decreased cluster P_{open} (Table VII).

TABLE VII

Gating Rate Constants for β-sandwich Core Constructs

Position	Construct	$\beta_2^{Choline}$	$\alpha_2^{Choline}$	β_2^{ACh}	α_2^{ACh}	L_2 ratio
Loop 1	R20L	365	2,119	—	—	3.589
	R20A	210	3,122			1.401
Loop 1	V29L	200	2,644	—	—	1.576
β1	V31A	276	2,728	—	—	2.108
	V31L	106	1,856			1.190
β1	L35A	182		—	—	1.565
	L35H	NFC				
	L35T	NFC				
	L35K	NFC	2,423			
β1	L40A	312	1,629	—	—	3.990
β2	V54L	124	1,340	—	—	1.928
β2	R55A	164	2,166	—	—	1.577
	R55W	98.2	2,894			0.707
β2	L56A	217	2,707	—	—	1.670
η1	L65V	124	2,166	—	—	1.193
	L65T	NFC				
Loop 4	P88A	NFC		—	—	
	P88E	NFC				
Loop 4	D89R	NFC		—	—	
	D89L	NFC				
β5′	L110V	70	1,874	—	—	0.778
β6	G114S	NFC				
	G114A	NFC				
β6	I116A	110	2,238	—	—	1.024
β6	P120G	—	—	49,531	2,006	0.988
β6′	A122L	358	2,142			3.482
β6′	S126V	—	—	40,253	1,770	0.910
	S126A			48,918	2,598	0.753
β7	S143T	118	2,200	—	—	1.117
	S143A	79	3,054			0.539
β7	M144L	917	2,911	—	—	6.563
	M144T	54	1,180			0.953
	M144I	93	2,823			0.686
	M144A	64	2,514			0.530
	M144S	—	—	20,546	3,604	0.228
	M144E	NFC				
	M144G	NFC				
	M144K	NFC				
β7	L146S	NFC				
	L146M	118	2,435	—	—	1.010
	L146F	97	2,234			0.905
β7	G147S	NFC		—	—	

$\beta_2^{Choline}$ and $\alpha_2^{Choline}$ were estimated from single-channel currents elicited by 20 and 0.4 mM choline, respectively. β_2^{ACh} and α_2^{ACh} were estimated from model-based kinetic analysis of clusters elicited at different concentrations of ACh. L_2 was calculated as the ratio β_2/α_2. "L_2 ratio" is the ratio of L_2 for the mutation and the wild-type. NFC denotes no functional channels either due to loss of expression or function or both.

nificantly lower than that of the TBS (0.931 ± 0.035; Grosman et al., 2000b) and loop 5 (0.936 ± 0.012; Chakrapani et al., 2003). Therefore, we conclude that the movement of loop 2 follows that of the TBS/loop 5 domain during channel opening. By combining the loop 2 results into a single REFER plot we have assumed that all of the residues in this loop move synchronously. The r-value for this plot was 0.98, which supports this assumption.

A REFER analysis of loop 7 is shown in Fig. 13 B. The overall Φ-value for loop 7 is 0.776 ± 0.034, with an r-value (0.99) that, again, supports the notion that the residues in this loop move in synchrony. This Φ-value is smaller than that of the TBS/loop 5 domain but is indistinguishable from that of loop 2 (Cymes et al., 2002). This suggests that during gating loop 2 and loop 7 move synchronously, and that this movement follows the movement of the TBS/loop 5 domain.

For those constructs that resulted in functional AChRs, point-mutations of the β-strands had only small effects on gating. The main exception was position M144 (on β-strand 7), and a REFER analysis of this site (Fig. 13 C) yielded a Φ-value of 0.841 ± 0.059. This suggests that during channel opening, conformational changes in this region of the β7 strand occur close in time to the movement of loop 2/loop 7. These mutations caused a <6.5-fold change in L_2 and, because the error in the Φ-estimate is likely to be large with such a small excursion in L_2, we cannot conclude with certainty whether this region moves marginally in advance of, or synchronously with, the loop 2/loop 7 domain.

We also performed a REFER analysis for the secondary gating mode of the F135A and Q140A mutants (Fig. 13 D). The Φ-value for these two sites was 0.374 ± 0.0. We do not understand the nature or functional consequence(s) of this reaction, but this observation suggests that loop 7 moves relatively late in this secondary gating reaction.

Finally, the β-strand mutation L40A increased L_2, but only by ~4-fold. A two-point REFER analysis of this position yields a Φ-value of 0.818. This residue is located in the vicinity of loop 2 and loop 7, and this Φ-value is consistent with the idea that this residue belongs to the loop 2/loop 7 gating domain.

DISCUSSION

We studied the kinetic behavior of 64 mutants (30 different residues) of the AChR α-subunit ECD. The diliganded channel-opening and -closing rate constants (and hence the equilibrium gating constant L_2) were estimated for all of these, and the closed-channel ligand-association and -dissociation rate constants (and hence the equilibrium dissociation constant K_d) were estimated in 13 constructs. This body of work concerning loop 2, loop 7, and the β-strands complements our previous studies of loop 5 (Chakrapani et al., 2003) and the EL/M2 (Grosman et al., 2000a) and provides a comprehensive view of the dynamic behavior of the EDC of the α-subunit during diliganded gating. We note that other regions of the α-subunit ECD still remain to be explored, including the NH_2 terminus, loops 8 and 10 on the "+" subunit interface, loops 6

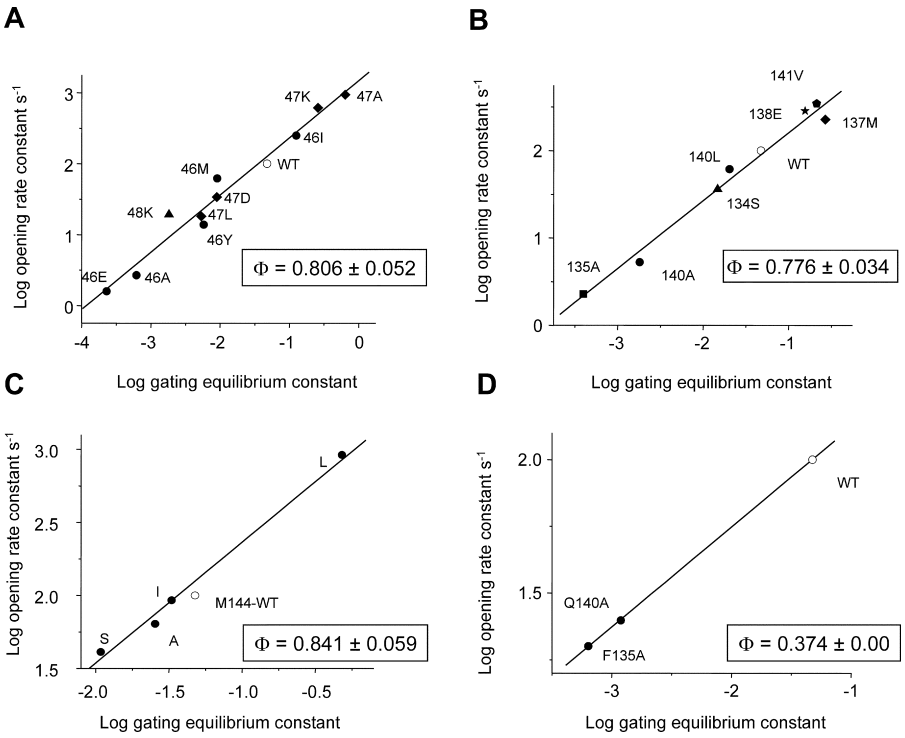

FIGURE 13. Rate-equilibrium free energy relationships. The y-axis is the log of the channel-opening rate constant, and the x-axis is the log of the diliganded-gating equilibrium constant. The Φ-values are the slopes of the linear fits ± SD. In all panels, the wt value is shown as an open circle. (A) The overall Φ-value for loop 2 is 0.81, which indicates that during diliganded opening this domain moves after the TBS and loop 5 (Φ = 0.93) but before residue αS269 (Φ = 0.69) in the EL/M2. (B) The Φ-value for the main gating reaction for loop 7 is 0.78. This value is indistinguishable from that of loop 2, thus these two domains move synchronously in the diliganded gating reaction. (C) The Φ-value for position αM144 is 0.84. We suspect that this residue moves in synchrony with loop 2 and 7. (B) The Φ-value for the secondary gating reaction for loop 7 is 0.37, which indicates that this domain moves relatively late in this reaction.

and 9 on the "−" subunit interface and the COOH-terminal tail that follows the M4 segment of the TMD.

There was no indication that any of the mutations that we studied in loop 2, loop 5, or the β-strands had a significant effect on agonist binding to closed AChRs. The central residue of the TBS is a tryptophan (αW149; Fig. 1). Previous results indicate that mutations of the apex of loop 5 (∼15 Å from αW149) or αD200 (∼10 Å from αW149) similarly do not alter the closed-channel K_d (Akk et al., 1996; Chakrapani et al., 2003). These results suggest that the affinity of the closed-state TBS for ACh is determined mainly by residues that are in the immediate vicinity of αW149. Exceptions include M1 residues αN217K (Wang et al., 1997) and εL221F (Hatton et al., 2003), both of which have been shown to influence agonist affinity but are distant from the TBS.

Although our exploration of desensitization was superficial, we did not observe any significant effect of any mutation on this process. The structural determinants of desensitization remain mysterious, but it seems that many residues of the TBS (Akk et al., 1999), loop 5 (Chakrapani et al., 2003), and, now, loop 2, loop 7, and the β-core are not significant players in this process.

The main focus of this report is the channel-gating reaction mechanism. Two different kinds of map emerge from our studies. First, the map of Φ-values provides a glimpse of the spatial organization and relative timing of the movements that occur during gating. Second, a map of the sensitivity of the equilibrium constant to perturbations (ΔG_0 in k_BT units, where k_B is the Boltzmann constant, T is the absolute temperature, and $\Delta G_0 = \ln[\text{mutant } L_2/\text{wt } L_2]$) suggests the extent of the participation of the perturbed region. It is, however, very difficult to draw firm conclusions from this second map. The relationship between energetic sensitivity and molecular motion is highly complex. In particular, whereas an effect of a mutation on the equilibrium constant implies motion, a negative result (no effect of a mutation) does not imply the lack of motion. If the environments of the side-chain were similar between C and O conformations, we would not expect to observe an effect on the reaction equilibrium constant, even if the residue had moved. In addition, we only examined a handful of substitutions at each position. Often, different side chains have extremely variable consequences, so the absence of an effect of one or two mutations does not necessarily imply insensitivity.

A change in L_2 can arise from a change in the unliganded equilibrium gating constant L_0, a change in the TBS closed/open equilibrium dissociation constant (K_d/J_d) ratio, or both. In loop 5, mutations increase L_2 specifically by increasing L_0 (Chakrapani et al., 2003), as is also the case for TMD residue δ268 (Grosman and Auerbach, 2000b). Therefore, we speculate that the changes in L_2 that were apparent with the loop 2, loop 7, and β-strand mutations also arise mainly or exclusively from parallel changes in L_0. Our conclusion that K_d is unaltered by many of these mutations supports this speculation, although direct measurements of J_d or L_0 are needed to confirm it definitively.

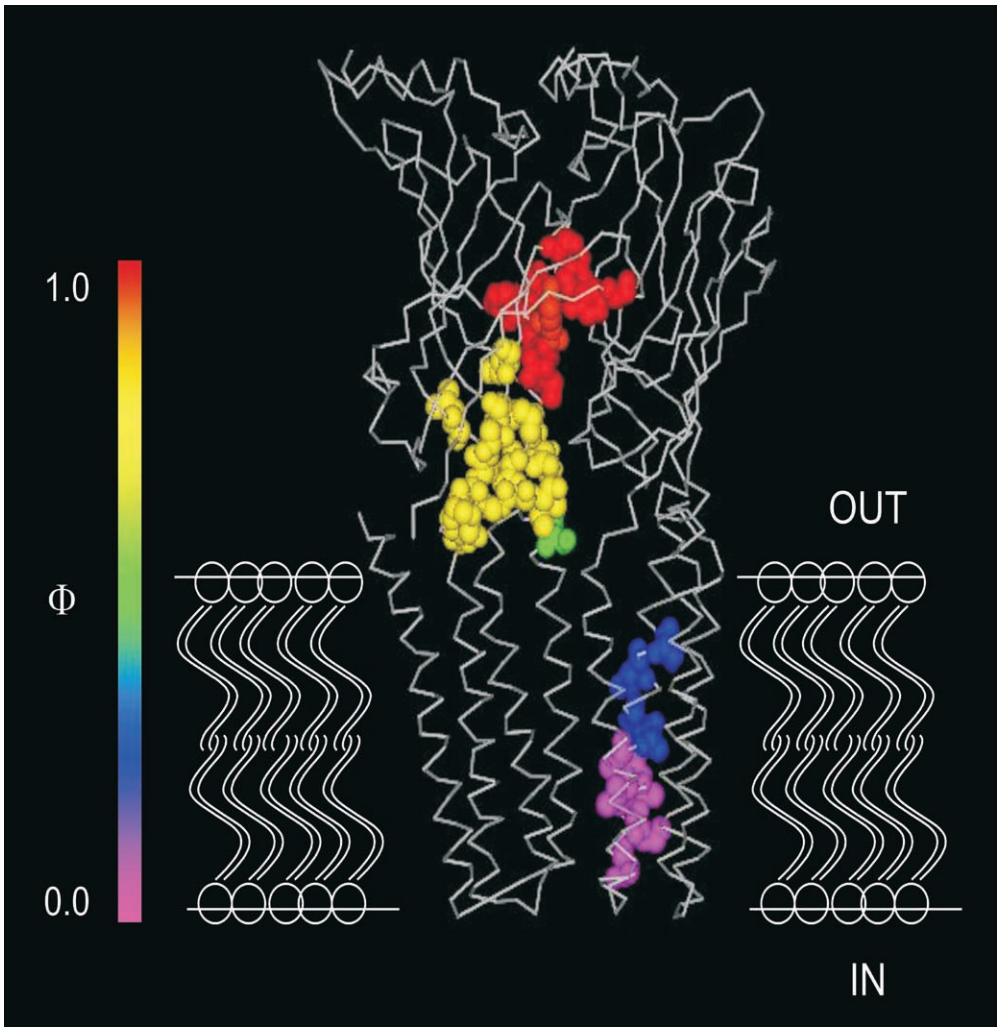

FIGURE 14. A Φ-map of the AChR. A model of the AChR (α- and δ-subunits) with residues color-coded according to their Φ-values for diliganded gating. The AChR is organized into contiguous, discrete, and synchronous domains that move sequentially, each as a rigid body, during gating. During channel opening, the TBS/loop 5 gating domain is the first to undergo a conformational change (red; Φ = 0.93), followed by the loop 2/loop 7/M144 gating domain (yellow; Φ = 0.80), followed by residue αS269 in the extracellular linker/αM2 (in green; Φ = 0.69), followed by the upper part of δM2 (blue; Φ = 0.32), and then the lower half of δM2 (magenta; Φ = 0.0). The extracellular domain is AChBP (Brejc et al., 2001) and the membrane domain is from *Torpedo* AChR (Miyazawa et al., 2003). The residues whose Φ-values were estimated independently are (Akk et al., 1996, 1999; Grosman et al., 2000a,b; Cymes et al., 2002; Chakrapani et al., 2003): αTBS (D200, D152, Y93, W149, Y198), αloop 5 (L92, Y93, N94, N95, A96, D97, G98, D99, F100), αloop 2 (V46, N47, Q48), αloop 7 (H134, F135, F137, D138, Q140, N141), rest of the αECD (L40, A122, M144), and δM2 (S258, I261, V263, L265, A266, S268, V269, L272, S274). Residues between those with similar Φ-values were given the same color code even though they were not measured experimentally.

Interestingly, the mutations of residues in loop 2, loop 7, and the EL, which all lie at the ECD-TMD interface, either increase or decrease L_2. This is in contrast to TMD/loop 5 mutations that mostly increase L_2 and TBS mutations that mostly decrease L_2. This suggests that in wt AChRs most TMD/loop 5 residues are optimized to increase the relative stability of the low-affinity, closed-channel conformation and that most TBS residues are optimized to increase the relative stability of the high-affinity, open-channel conformation. The interfacial loop 2/loop 7/EL residues are in between these extremes.

In single positions that have been mutated extensively—for example, αD97 (n = 17 side chains), αN47 (n = 4), αM144 (n = 8) and δS268 (n = 12)—there is no unambiguous correlation between the magnitude of the effect on L_2 and the chemical properties of the side chain. Without explicit structural information and when only a handful of substitutions of a given residue are examined, caution must be exercised in this aspect of relating structure to function.

Anomalous Gating Behaviors

We observed two kinetic behaviors that are unusual and can therefore be characterized as "anomalous". First, in two of the loop 7 constructs, F135A and Q140A, there were two diliganded open states. In both of these mutants, our analyses indicate that the two open states are uncoupled and arise as independent gating reactions from the diliganded-closed state. Sine and coworkers also observed two open states in a TMD (αM3) mutation, although their studies led them to conclude that the two open states are coupled (Wang et al., 1999). The functional significance (if any) and the structural correlates of this secondary gating reaction are not quite clear. However, the low Φ-values for the loop 7 mutants for this reaction (Φ = 0.37) suggest that this

domain is mostly closed-like at the transition state of this reaction whereas it is mostly open-like at the transition state for the main gating reaction ($\Phi = 0.77$).

The second anomalous kinetic behavior pertains to construct Q48A, in loop 2. This substitution increased both the channel opening and closing rate constants. A two-point REFER analysis gives a Φ-value of 1.6, which suggests a "catalytic" effect wherein the mutation stabilized the transition state to an extent greater than expected solely from the change in the relative stability of the ground states. Although some of the scatter in REFER plots from other sites undoubtedly arises from small catalytic effects (see Grosman et al., 2000b, for an example), in AChR diliganded gating large violations of the essential REFER assumption are rare. Of the >100 positions that we have examined overall, so far only αQ48A and δA266T, L and N, which is near the middle of the δM2 segment (Cymes et al., 2002), show extreme versions of this anomalous behavior. As yet, we are unable to discern a pattern for this behavior with respect either to location in the AChR or side chain properties relative to the wt.

Relevance to Proposed Gating Mechanisms

Our study supports the hypothesis that loop 2 and 7 are dynamic modules that couple agonist binding in the extracellular domain (specifically, the movement of the TBS/loop 5 domain) to the conformational changes in the EL/M2 and the membrane domain (Kash et al., 2003; Miyazawa et al., 2003). Our results shed additional light on these proposed gating reaction mechanisms.

In $GABA_A$ receptors, charge reversal mutations increased the EC_{50} of the agonist, which led to the proposal that an electrostatic interaction between D57 (N47 in the AChR) in loop 2 with K279 (S266) in the EL/M2 is a component of the relay of the gating conformational change (Kash et al., 2003). In our experiments there was no correlation between the charge or volume of the N47 side chain and the effects on L_2 (Fig. 4). Hence, an electrostatic interaction between loop 2 and other regions of the protein is not likely to be a general gating mechanism that pertains to AChRs. However, in our studies we have not probed the role of an adjacent residue E45, hence the involvement of E45 in an electrostatic interaction with loop 7 and EL cannot be ruled out.

Along similar lines of evidence, an electrostatic interaction between the conserved D138 in loop 7 with the EL/M2 was proposed to be a critical element of gating in both $GABA_A$ and glycine receptors (Schofield et al., 2003). In our experiments, mutating the corresponding residue (D138) to A and K caused a complete loss of activity (expression, gating, or both), whereas a charge-conserving mutation (E) increased L_2 by threefold. While these results are consistent with the proposed loop 7–EL/M2 electrostatic interaction, a more extensive mutational scan is needed to further explore this hypothesis.

Based on electron microscope images of *Torpedo* AChRs, it has been suggested that the loop 2 residue V46 participates in a hydrophobic interaction with the EL/M2 to drive channel gating (Miyazawa et al., 2003). Although these images are not at atomic resolution, this "pin-into-socket" interaction was proposed as the only apparent direct structural link between the ECD and the TMD. In this model, a rotational movement of the inner β-sheet, brought about by agonist binding, is communicated through loop 2 to the M2 helices, which in turn relays its motion to a hydrophobic girdle that forms the "gate" of the channel.

We studied five side chain substitutions of varying hydrophobicity for α-subunit loop 2 residue V46. Mutation to I (more hydrophobic) increased L_2, and mutation to Y, A, or E (less hydrophobic) decreased L_2. However, mutation to M (more hydrophobic) also decreased L_2. We suspect that side chain hydrophobicity is one factor that determines L_2, but that other factors (such as side chain volume) also come into play. Further structural, mutational, and computational studies should help define the interaction sites and parameters more precisely.

From a comparison of electron images of AChRs (with and without agonist) and the structure of AChBP, Unwin and coworkers have suggested that the agonist-mediated channel opening involves 15° rotations of the inner β-sheets of α-subunit, about an axis passing through the disulfide bridge and normal to the plane of the membrane (Unwin et al., 2002). In this proposed mechanism the maximum relative displacement of the β-sheets occurs at midlevel, where the inner-sheet curls around to meet the outer sheet. If these structural changes are accompanied by changes in the local side chain environments we would expect to observe effects on the gating equilibrium constant consequent to the mutation of these residues. However, of the 26 mutations in this region of the α-subunit (L35, L40, V54, R55, L56, P120, A122, S126, S143, M144, L146) only three (M144L, M144S, and L40A) had even a modest effect on L_2 (7-, 4-, and 4-fold, respectively, with mutations in both α-subunits). These results suggest that these side chains do not experience a significant change in their local environments when the channel switches from a closed to an open conformation. However, for a residue that moves during gating, if the local environment of the side chain remains constant between "closed" and "open" positions we would not expect to detect a change in L_2. Our results are inconsistent with the β-sheet rotation hypothesis, but they cannot be taken as absolute proof against it.

The β-core is comprised mainly of hydrophobic amino acids. Our results show that AChRs are highly sensitive to polar side-chain substitution at residues in this domain. An examination reveals that all of the mutations (except G114A) that led to loss of activity involved substitutions with a more polar side-chain. G114 is present at the start of the β6 strand where the β5′-β6 loop turns and hence this position may be sensitive to any side-chain substitution.

M144 is a part of the β7 strand, which supports loop 8 and W149 (the "floor" of the TBS). Of the eight mutations investigated at this position two (M144L and M144S) had a modest effect on L_2 (seven- and fourfold respectively), three had no significant effect on L_2, and three failed to show activity. Interestingly, in M144S the agonist association and dissociation rate constants were unaltered, which again emphasizes the local nature of the determinants of agonist affinity.

The Dynamic Organization of Gating

Fig. 14 shows a map of diliganded-gating Φ-values for the α-subunit ECD and the δ-subunit TMD (Cymes et al., 2002). So far, the ECD regions that have been mapped are the TBS (Grosman et al., 2000b), loop 5 (Chakrapani et al., 2003), loop 2, loop 7, the β-core, and part of the EL/M2 (Grosman et al., 2000a).

This map has several notable features. First, there is a spatial gradient of Φ-values, from ∼1 at the TBS to ∼0 below the middle of the membrane in the δ-subunit. This pattern led to the proposal that AChR gating occurs as a reversible "conformational wave", wherein the movements of TBS residues precede those of the membrane domain during channel opening (Grosman et al., 2000b). Φ-maps of other AChR regions, most notably the α-subunit TMD, are needed to complete and perhaps modify this view of gating.

Second, the map appears to be organized into discrete, contiguous domains within which all of the residues have the same Φ-value. This suggests that the gating "conformational wave" is granular. The uniformity of the Φ-value within a domain implies that the atoms move synchronously, i.e., as a rigid body. The residues in the TBS/loop 5 domain all have $\Phi = 0.93$. Those in the loop 2/loop 7 domain have $\Phi = 0.80$. One residue in the EL/M2 (αS269I) has $\Phi = 0.69$ (Grosman et al., 2000a). Residues in the upper-half of δM2 have $\Phi = 0.32$, whereas those in the lower half have $\Phi = 0.0$ (Cymes et al., 2002). Although the spatial boundaries of these domains have not been fully explored, it appears that they each span ∼10–20 Å and consist of on the order of dozens of residues.

It is important to consider whether or not the gating domains are indeed discrete. Φ-values measurements are inherently imprecise when the changes in L_2 are small (Cymes et al., 2002), and they fail to provide information on the relative sequences of motion as they approach at their saturation limits, 0 and 1. In addition, the atomic structure of AChRs is still not known. It is therefore difficult to establish with certainty whether the Φ-values we have measured in AChR gating define discrete structural entities.

Our results suggest that they do. For example, in AChBP the C_β atom of W153 (αW149 in the AChR, at the heart of the TBS) and the C_δ carbon of I92 (the apex of loop 5) are separated by 18 Å, yet these two sidechains in AChRs both have $\Phi = 0.93$. In contrast, this atom of I92 in AChBP and the C_β atom of N47 (in loop 2) approach within 8 Å, yet in the AChR these two side-chains have distinct Φ-values (0.93 and 0.81). More dramatically, recent structural analyses of the transmembrane region (Miyazawa et al., 2003) indicates that atoms of the M2 12′ and 10′ side-chains might be separated by <5.0 Å, but kinetic analyses indicate that in the δ-subunit these two positions belong to distinct domains with $\Phi = 0.3$ and 0.0, respectively (Cymes et al., 2002). Although the structure of the AChR needs to be refined, the current evidence suggests that AChR residues are organized into discrete, contiguous, synchronously-moving gating domains.

We hypothesize that the occupancy of the TBS by an agonist induces a local structural "defect" that causes the TBS/loop 5 gating domain to move as a rigid body. This movement, in turn, induces a localized structural defect(s) in the adjacent loop 2/loop 7 domain (and perhaps elsewhere), which then moves. The loop 2/loop 7 movement is coupled to the movement of the EL/M2 domain, and so on. In this mechanism, gating occurs as the stepwise propagation, or diffusion, of a conformational defect through the protein, eventually linking localized structural changes at the TBS consequent to ligand binding with localized conformational changes in the pore that regulate ionic conduction.

Our results suggest that the reversible AChR gating "conformational wave" arises from the coupled movements of a few kinematic elements. We speculate that each element can adopt an "active" or "inactive" conformation, with the probability of being "active" depending on the status of its neighbors. Although a protein with N two-state gating domains can adopt 2^N conformations, coupling between domains could constrict the conformational space to only N + 1 sequentially-occupied states. Such an organized, linked, motion of rigid bodies may serve to quicken the dynamics of the AChR allosteric conformational change.

Olaf S. Andersen served as editor.

Submitted: 22 December 2003
Accepted: 3 March 2004

REFERENCES

Akk, G., S. Sine, and A. Auerbach. 1996. Binding sites contribute unequally to the gating of mouse nicotinic alpha D200N acetyl-

choline receptors. *J. Physiol.* 496:185–196.

Akk, G., M. Zhou, and A. Auerbach. 1999. A mutational analysis of the acetylcholine receptor channel transmitter binding site. *Biophys. J.* 76:207–218.

Auerbach, A., and G. Akk. 1998. Desensitization of mouse nicotinic acetylcholine receptor channels. A two-gate mechanism. *J. Gen. Physiol.* 112:181–197.

Brejc, K., W.J. van Dijk, R.V. Klaassen, M. Schuurmans, J. van Der Oost, A.B. Smit, and T.K. Sixma. 2001. Crystal structure of an ACh-binding protein reveals the ligand-binding domain of nicotinic receptors. *Nature.* 411:269–276.

Chakrapani, S., T.D. Bailey, and A. Auerbach. 2003. The role of loop 5 in acetylcholine receptor channel gating. *J. Gen. Physiol.* 122:521–539.

Changeux, J.P., and S.J. Edelstein. 1998. Allosteric receptors after 30 years. *Neuron.* 21:959–980.

Colquhoun, D., and B. Sakmann. 1998. From muscle endplate to brain synapses: a short history of synapses and agonist-activated ion channels. *Neuron.* 20:381–387.

Corringer, P.J., N. Le Novere, and J.P. Changeux. 2000. Nicotinic receptors at the amino acid level. *Annu. Rev. Pharmacol. Toxicol.* 40:431–458.

Cymes, G.D., C. Grosman, and A. Auerbach. 2002. Structure of the transition state of gating in the acetylcholine receptor channel pore: a phi-value analysis. *Biochemistry.* 41:5548–5555.

Fernando Valenzuela, C., P. Weign, J. Yguerabide, and D.A. Johnson. 1994. Transverse distance between the membrane and the agonist binding sites on the *Torpedo* acetylcholine receptor: a fluorescence study. *Biophys. J.* 66:674–682.

Galzi, J.L., F. Revah, D. Black, M. Goeldner, C. Hirth, and J.P. Changeux. 1990. Identification of a novel amino acid alpha-tyrosine 93 within the cholinergic ligands-binding sites of the acetylcholine receptor by photoaffinity labeling. Additional evidence for a three-loop model of the cholinergic ligands-binding sites. *J. Biol. Chem.* 265:10430–10437.

Grosman, C., and A. Auerbach. 2000a. Asymmetric and independent contribution of the second transmembrane segment 12′ residues to diliganded gating of acetylcholine receptor channels: a single-channel study with choline as the agonist. *J. Gen. Physiol.* 115:637–651.

Grosman, C., and A. Auerbach. 2000b. Kinetic, mechanistic, and structural aspects of unliganded gating of acetylcholine receptor channels: a single-channel study of second transmembrane segment 12' mutants. *J. Gen. Physiol.* 115:621–635.

Grosman, C., and A. Auerbach. 2001. The dissociation of acetylcholine from open nicotonic receptor channels. *Proc. Natl. Acad. Sci. USA.* 98:14102–14107.

Grosman, C., F.N. Salamone, S.M. Sine, and A. Auerbach. 2000a. The extracellular linker of muscle acetylcholine receptor channels is a gating control element. *J. Gen. Physiol.* 116:327–340.

Grosman, C., M. Zhou, and A. Auerbach. 2000b. Mapping the conformational wave of acetylcholine receptor channel gating. *Nature.* 403:773–776.

Hatton, C.J., C. Shelley, M. Brydson, D. Beeson, and D. Colquhoun. 2003. Properties of the human muscle nicotinic receptor, and of the slow-channel myasthenic syndrome mutant epsilonL221F, inferred from maximum likelihood fits. *J. Physiol.* 547:729–760.

Horenstein, J., D.A. Wagner, C. Czajkowski, and M.H. Akabas. 2001. Protein mobility and GABA-induced conformational changes in GABA(A) receptor pore-lining M2 segment. *Nat. Neurosci.* 4:477–485.

Itzhaki, L.S., D.E. Otzen, and A.R. Fersht. 1995. The structure of the transition state for folding of chymotrypsin inhibitor 2 analysed by protein engineering methods: evidence for a nucleation-condensation mechanism for protein folding. *J. Mol. Biol.* 254: 260–288.

Jackson, M.B., B.S. Wong, C.E. Morris, H. Lecar, and C.N. Christian. 1983. Successive openings of the same acetylcholine receptor channel are correlated in open time. *Biophys. J.* 42:109–114.

Karlin, A. 2002. Emerging structure of the nicotinic acetylcholine receptors. *Nat. Rev. Neurosci.* 3:102–114.

Kash, T.L., A. Jenkins, J.C. Kelley, J.R. Trudell, and N.L. Harrison. 2003. Coupling of agonist binding to channel gating in the GABA(A) receptor. *Nature.* 421:272–275.

Maconochie, D.J., and J.H. Steinbach. 1998. The channel opening rate of adult- and fetal-type mouse muscle nicotinic receptors activated by acetylcholine. *J. Physiol.* 506:53–72.

Miyazawa, A., Y. Fujiyoshi, M. Stowell, and N. Unwin. 1999. Nicotinic acetylcholine receptor at 4.6 A resolution: transverse tunnels in the channel wall. *J. Mol. Biol.* 288:765–786.

Miyazawa, A., Y. Fujiyoshi, and N. Unwin. 2003. Structure and gating mechanism of the acetylcholine receptor pore. *Nature.* 424: 949–955.

Qin, F., A. Auerbach, and F. Sachs. 1996. Estimating single-channel kinetic parameters from idealized patch-clamp data containing missed events. *Biophys. J.* 70:264–280.

Salamone, F.N., M. Zhou, and A. Auerbach. 1999. A re-examination of adult mouse nicotinic acetylcholine receptor channel activation kinetics. *J. Physiol.* 516:315–330.

Schofield, C.M., A. Jenkins, and N.L. Harrison. 2003. A highly conserved aspartic acid residue in the signature disulfide loop of the alpha 1 subunit is a determinant of gating in the glycine receptor. *J. Biol. Chem.* 278:34079–34083.

Shen, X.M., K. Ohno, A. Tsujino, J.M. Brengman, M. Gingold, S.M. Sine, and A.G. Engel. 2003. Mutation causing severe myasthenia reveals functional asymmetry of AChR signature cystine loops in agonist binding and gating. *J. Clin. Invest.* 111:497–505.

Ternstrom, T., U. Mayor, M. Akke, and M. Oliveberg. 1999. From snapshot to movie: phi analysis of protein folding transition states taken one step further. *Proc. Natl. Acad. Sci. USA.* 96:14854–14859.

Unwin, N. 2000. The Croonian Lecture 2000. Nicotinic acetylcholine receptor and the structural basis of fast synaptic transmission. *Philos. Trans. R. Soc. Lond. B Biol. Sci.* 355:1813–1829.

Unwin, N., A. Miyazawa, J. Li, and Y. Fujiyoshi. 2002. Activation of the nicotinic acetylcholine receptor involves a switch in conformation of the alpha subunits. *J. Mol. Biol.* 319:1165–1176.

Villegas, V., J.C. Martinez, F.X. Aviles, and L. Serrano. 1998. Structure of the transition state in the folding process of human procarboxypeptidase A2 activation domain. *J. Mol. Biol.* 283:1027–1036.

Wang, H.L., A. Auerbach, N. Bren, K. Ohno, A.G. Engel, and S.M. Sine. 1997. Mutation in the M1 domain of the acetylcholine receptor alpha subunit decreases the rate of agonist dissociation. *J. Gen. Physiol.* 109:757–766.

Wang, H.L., M. Milone, K. Ohno, X.M. Shen, A. Tsujino, A.P. Batocchi, P. Tonali, J. Brengman, A.G. Engel, and S.M. Sine. 1999. Acetylcholine receptor M3 domain: stereochemical and volume contributions to channel gating. *Nat. Neurosci.* 2:226–233.

Zhou, M., A.G. Engel, and A. Auerbach. 1999. Serum choline activates mutant acetylcholine receptors that cause slow channel congenital myasthenic syndromes. *Proc. Natl. Acad. Sci. USA.* 96:10466–10471.